



Ecological Niche Modeling of the Endemic Himalayan Near-Threatened Treeline Conifer *Abies spectabilis* (D.Don) Mirb. in the Indian Central Himalaya

10

Siddhartha Kaushal , Sharanjeet Kaur , Anshu Siwach , Prachi Sharma , Prem Lal Uniyal , Rajesh Tandon , Shailendra Goel , K. S. Rao , and Ratul Baishya

Abstract

Abies spectabilis (D.Don) Mirb. is an endemic Himalayan near-threatened coniferous species and the predominant treeline-forming species in the Indian Central Himalaya (Uttarakhand). The impact of climate change and anthropogenic activities is perilous to its habitat distribution. Accurate species habitat distribution is a prerequisite for efficient conservation planning. This vital information is still missing in the Indian Himalayan region for *A. spectabilis*. This study models the habitat suitability of *A. spectabilis* in Uttarakhand and discusses the management implications. Species occurrence records from primary and secondary sources were used with environment variables for habitat suitability modeling using the MaxEnt approach. Environment variables included bioclimatic (BCVs), topographic, edaphic, and anthropogenic variables. The BCVs from two global bioclimatic databases CHELSA (model 1) and WorldClim (model 2) were used. Models were validated using threshold-independent measures and further used to build habitat suitability maps. Both models performed optimally; however, model 2 had higher average values for the area under the curve (AUC) (0.980), partial AUC (0.977), and the AUC ratio (1.954) indicating higher predictive power. The precipitation of the driest month (BIO14) was the most important predictor variable under both models. The habitat suitability area for model 1 (16,324.57 km²) was five times greater than model 2 (3323.86 km²). Only 826.86 km² area (model 2) was highly suitable for *A. spectabilis*. The habitat

Supplementary Information The online version contains supplementary material available at https://doi.org/10.1007/978-981-99-0131-9_10.

S. Kaushal · S. Kaur · A. Siwach · P. Sharma · P. L. Uniyal · R. Tandon · S. Goel · K. S. Rao · R. Baishya (✉)
Department of Botany, University of Delhi, Delhi, India
e-mail: rbaishya@botany.du.ac.in

© The Author(s), under exclusive license to Springer Nature Singapore Pte Ltd. 2023

S. Dhyani et al. (eds.), *Ecosystem and Species Habitat Modeling for Conservation and Restoration*, https://doi.org/10.1007/978-981-99-0131-9_10

181

suitability is concentrated predominantly in a tight group in the northern region of Uttarakhand. Chamoli (8.43%), Rudraprayag (6.20%), and Uttarkashi (0.53%) were the top 3 districts with the highest percentage of high suitability regions under model 2. The results from the habitat suitability distribution of *A. spectabilis* suggest in situ conservation of present occurrences and monitoring of the regeneration process. Stringent monitoring in the protected areas and the highly suitable habitat regions modeled must be used for assisted regeneration and plantation-based habitat enhancement of this endangered species.

Keywords

CHELSA · WorldClim · MaxEnt · *Abies spectabilis* · Alpine treeline · Uttarakhand

10.1 Introduction

Globally mountains cover ca. 25% of the land surface and act as a habitat for around 12% of the global population. Mountain ecosystems provide a range of services and are important from socioeconomic and cultural perspectives. They are the predominant source of freshwater and the head source of prominent rivers around the globe (Grabherr and Messerli 2011). Various climatic zones resulting from latitudinal zonation are condensed within the mountains, making them unique ecosystems supporting various climate zones and associated biodiversity. The steep slope and elevational gradients create unique biodiversity hotspots for various life forms. Moreover, the transition zones along the elevational gradient create ecotones, increasing the number of endemic species in the mountains (Diaz et al. 2003). Half of the global biodiversity hotspots are in the mountainous regions, representing the enormity of mountain biodiversity (Rodríguez-Rodríguez and Bomhard 2011).

Globally the impact of climate change is not uniform; mountain ecosystems especially high-elevation mountain ecosystems are acknowledged as the pioneers in expressing climate change impacts (Becker and Bugmann 2001). In contrast with the pre-industrialized temperature, the 1.3 °C to 1.6 °C increase in surface air temperature over land is one of the most recognized impacts of climate change. The elevation-dependent climatic zones on mountains undergo rapid transitions due to steep slopes and elevational gain; moreover, the high-elevation regions are relatively undisturbed from strong anthropogenic influence, making the mountain ecosystems vulnerable to climate change-induced warming impacts (Beniston 2003). In this regard, mountain ecosystems are even debated as the sentinels of climate change, especially the high-elevation treeline ecotone regions and the alpine vegetation, though there are several biotic, abiotic, and spatial complications in this regard (Malanson et al. 2019). Upward movement of treeline species and alpine flora or even changes in the composition of alpine flora is a recognized impact of climate

change on mountain ecosystems; the upward movement of the species is to remain associated with their bioclimatic preference (Zisenis and Price 2011; IPCC 2019).

For the decade 2006–2015, in context with the pre-industrialization period, the global mean surface (land and ocean) temperature increase was around 0.87 °C (Allen et al. 2019). From 1901 to 2009, the annual mean temperature in India increased by 0.56 °C (Attri and Tyagi 2010), the year 2016 in India was recorded as the warmest year with a temperature increase of 0.71 °C, and the year 2020 was the eighth warmest in record since the year 1901 (Attri and Chug 2021). The Himalayan mountain ranges are experiencing a more significant impact and are warming faster than other mountain ranges globally. The Himalayas showed a significant increase in annual temperature along with a reduced number of cold days and nights than the global trend, an increase in decadal temperature rise with a positive association with elevation, temporal variation in warming, rainfall deficit, pre-monsoon drought, early snowmelt, and extreme rainfall events (Schickhoff et al. 2016). The northwestern region of the Himalayas has warmed by almost 1.1 °C in the past century (Bhutiyan 2015). Additionally, the rapid population boom leading to widespread modern construction is causing increased regional warming in the Himalayas (Pandit 2013).

The high-elevation Himalayan treeline ecotone is represented by 58 tree species (Singh et al. 2020). The treeline taxa having a specialist niche might face extirpation due to competition from the upward migration of lowland species, alpine shrubs, and krummholz species (Schickhoff et al. 2015). In the Indian Himalayan region (IHR), limited studies have investigated the impact of real-time climate change on treeline dynamics using tree rings with chronologies. Yadava et al. (2017) reported an average upward shift of 11–54 m decade⁻¹ of the Himalayan pine (*Pinus wallichiana* A.B. Jacks.) treeline in the western Himalaya; the winter and early spring warming due to climate change resulted in the increased radial growth. Similarly, Singh et al. (2018) showed elevated monthly temperature during November and February to positively correlate with increased radial growth in Himalayan silver fir, i.e., *Abies spectabilis* (D. Don) Mirb., during the past century. Interestingly, the studies independently also attributed anthropogenic pressure as a regulatory factor in treeline dynamics.

Conservation planning of Himalayan treeline species, therefore, becomes crucial. Ecological niche modeling (ENM) is a requisite tool for the conservation planning approach, not only for current distribution but also for future distribution under various climate change scenarios (McShea 2014). Globally several studies have incorporated the use of ENM for plant species conservation planning (Zhang et al. 2012; Nakao et al. 2013; Fajardo et al. 2014; Spiers et al. 2018). From the IHR perspective, ENM has been used for the conservation planning of endangered plant species (Adhikari et al. 2019; Dhyani et al. 2021), medicinal plants (Yang et al. 2013; Tariq et al. 2021), endemic species (Chitale and Behera 2019; Manish and Pandit 2019), major tree species (Chakraborty et al. 2016), prominent shrub species (Dhyani et al. 2018), invasive plant species (Srivastava et al. 2018), and several others. These studies and others (Ugupta et al. 2015; Manish et al. 2016; Dhyani et al. 2020) have also focused on the potential distribution under future climate

scenarios to provide appropriate management implications concerning climate change. However, in terms of treeline ecotone, there are very few studies on the IHR (Singh et al. 2012, 2021a). Those present focus primarily on broadleaf species, viz., *Betula utilis* D. Don (Singh et al. 2013, 2021b; Hamid et al. 2019) and *Quercus semecarpifolia* Sm. (Singh et al. 2021c).

The dominant timberline species of the Indian Central Himalaya (ICH) which is represented by the Uttarakhand state (Nandy et al. 2009; Negi 2022) are *Q. semecarpifolia*, *B. utilis*, *Abies pindrow* (Royle ex D. Don) Royle, and *A. spectabilis* (Negi et al. 2018; Rawal et al. 2018; Sharma et al. 2018; Tiwari et al. 2018). Among these species, *A. spectabilis* is rated as near threatened as per the IUCN Red List Criteria (Zhang et al. 2011). Though both *A. spectabilis* and *A. pindrow* are treeline species, only *A. spectabilis* generally forms the treeline in ICH, while *A. pindrow* remains a few hundred meters below (Singh et al. 2020). This makes *A. spectabilis* the only coniferous timberline – treeline-dominant forest-forming tree species in ICH. The treeline of *A. spectabilis* in the Tungnath region which lies in the ICH recorded no upward shift for the past four decades (Singh et al. 2018). Kaushal et al. (2021) showed unimodal girth class distribution of *A. spectabilis* in the Tungnath region, indicating long-term poor regeneration in the region; such distribution is perilous for the future security of this endemic Himalayan species. Poor natural regeneration of *A. spectabilis* in ICH was noted by several others; the primary reasons are anthropogenic pressure, land-use change, and winter warming trend (Rai et al. 2012a; Singh et al. 2018, 2019).

The facts mentioned above led us to choose ICH and *A. spectabilis* for the present study. For efficient management and planning of conservation strategies, it is imperative to precisely model the habitat distribution of *A. spectabilis*, which is still eluded in ICH. Our study, therefore, addresses the following broad objectives: (1) determination of an appropriate global bioclimatic database, (2) identifying the most influential climatic and non-climatic predictor variables, (3) determining the currently suitable area of *A. spectabilis* in ICH, and (4) considering necessary management implications for conservation planning.

10.2 Materials and Methods

10.2.1 Study Area and Tree Species of Interest

The study area is the Uttarakhand state of India, which constitutes the central portion of the Indian Himalayan region (Fig. 10.1). Uttarakhand, also known as Devbhumi or the land of gods/goddesses, lies between 28°43' N to 31°27' N latitude and 77°34' E to 81°02' E longitude and has a wide elevational span from 187 m.a.s.l. to 7816 m. a.s.l. The state is bordered internationally in the north by China and in the east by Nepal. On the western and southern sides, it is bordered by interstate boundaries of Himachal Pradesh and Uttar Pradesh, respectively. The state covers an area of 53,483 km² of which 71.05% (38,000 km²) is recorded as forest area. The average rainfall of the state for the year 2019 was 1644 mm, while the minimum and the

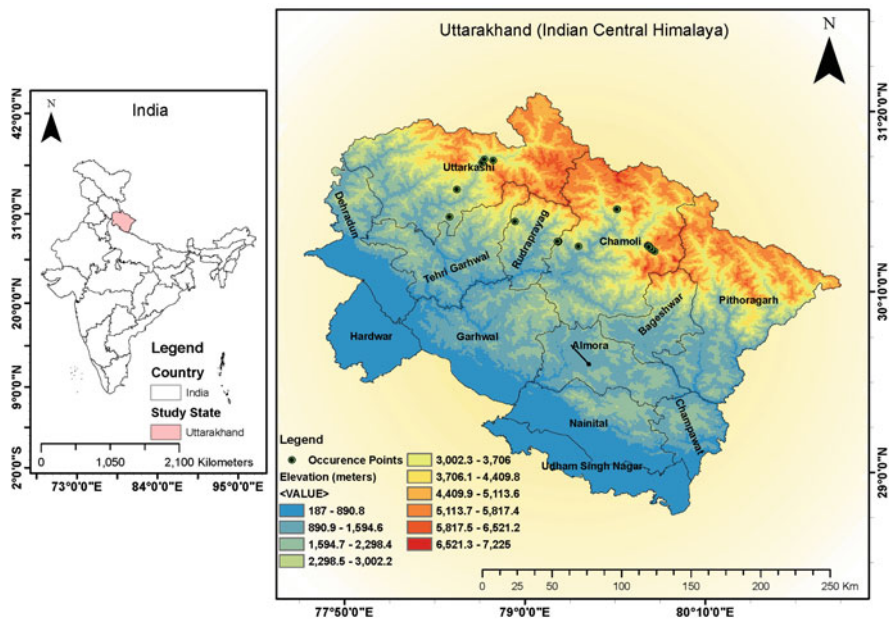


Fig. 10.1 Study area map representing the location of Uttarakhand in India and an elevational gradient map showing the distribution of *Abies spectabilis* occurrence records

maximum temperatures recorded were -2.9°C and 40.7°C , respectively (FSI 2019; Uttarakhand at a Glance 2020).

This study focuses on an endemic Himalayan near-threatened tree species *Abies spectabilis* (D.Don) Mirb. (Family: Pinaceae) (Fig. 10.2). The English vernacular name of the species is Himalayan silver fir, while locally in Central Himalaya it is known as Morinda or Raga. It is an evergreen tree species that attain heights of up to 45 m. The wood is of commercial value in construction and carpentry, while the decoction of the leaves and bark is antipyretic and is used to treat respiratory problems. The elevational range limit of this species is from 2400 m to 4000 m and is predominantly found on the northern to northwestern slopes between 3000 m and 4000 m. The native habitat distribution of the species ranges from Afghanistan to the Karakoram range, Jammu and Kashmir, Himachal Pradesh, Uttarakhand, Tibet, and Nepal (Gaur 1999; Zhang et al. 2011).

10.2.2 Species Occurrence Data

Gathering the species occurrence data for *A. spectabilis* is challenging since it is a treeline coniferous species. It occurs near ridge tops or high-elevation regions with undulating terrain, extreme climatic events, and poor accessibility. Even in the Global Biodiversity Information Facility database (GBIF), there were only

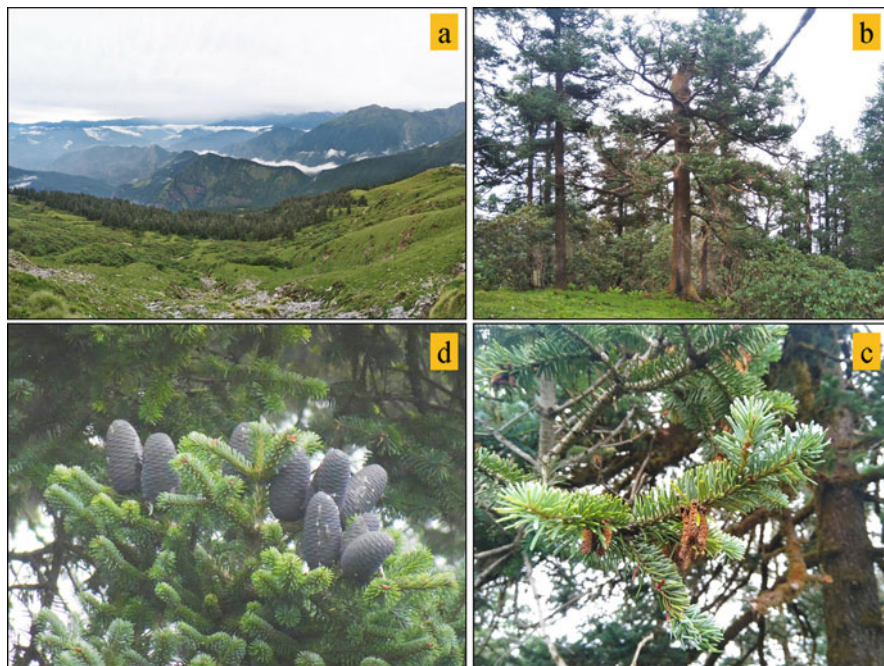


Fig. 10.2 *Abies spectabilis* habitat. (a) *A. spectabilis* treeline at Tungnath, Uttarakhand. (b) Mature *A. spectabilis* tree; notice the thick *Rhododendron campanulatum* D. Don krummholz in the understory. (c) A twig-bearing pollen cones. (d) Mature female cones of *A. spectabilis*

13 records of *A. spectabilis* from India with geo-coordinates. Only one record pertained to the area of interest in this study (GBIF 2022). We conducted our field survey in the Tungnath region, which lies in the core zone of the Kedarnath Wildlife Sanctuary in the Rudraprayag district of Uttarakhand. We recorded the geo-coordinate data for *A. spectabilis* occurrence using a hand-held Global Positioning System (GPS) meter (Garmin® GPS72™). Additionally, we enhanced our occurrence records with 15 occurrence points from published literature (Supplementary Table 10.1).

A total of 26 occurrence records were collected using primary (11 occurrence points) as well as secondary sources (15 occurrence points) (Supplementary Table 10.1, Fig. 10.1). The occurrence points were converted to a shapefile and projected to WGS84 projection using SDMtoolbox (version 2.5) (Brown et al. 2017) in ArcGIS (version 10.5). There were spatial clusters in occurrence points (Fig. 10.3); such clusters lead to spatial autocorrelation and biasedness in model predictions causing inflated values for model accuracy (Veloz 2009). Occurrence points were therefore spatially rarefied using a 1-km resolution using *spatially rarefy occurrence data* tool under SDMtoolbox. A 1-km resolution was selected due to small occurrence records. The distribution range of *A. spectabilis* is narrow, and the

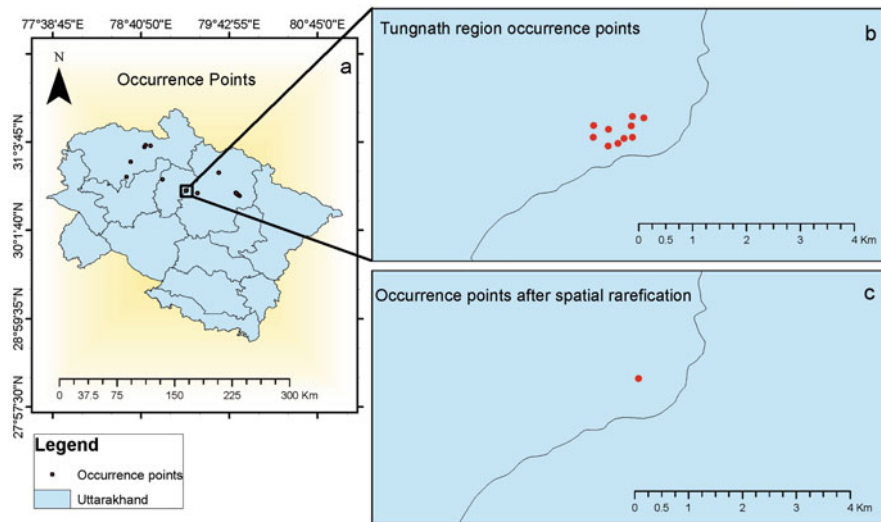


Fig. 10.3 Spatial rarefaction of occurrence records. (a) Occurrence records of *A. spectabilis* in Uttarakhand. (b) One example of spatial clustering of occurrence records in the Tungnath region. (c) Occurrence records after spatial rarefaction (resolution 1 km)

environmental layers we selected were of 30 arc-second resolution (ca. 1 km × 1 km resolution).

10.2.3 Environmental Data for Habitat Distribution Modeling

A total of 44 environmental variables were used including climatic (19 WorldClim bioclimatic variables + 19 CHELSA bioclimatic variables + 1 solar radiation variable), topographic (3), edaphic (1), and anthropogenic (1) variables. For climatic variables, we choose the bioclimatic variables (BCVs), which are the derivatives of monthly temperature and precipitation values that determine habitat distribution and its abundance and interactions (Noce et al. 2020). For mountainous regions having sharp climate gradients due to their topography, capturing the environmental variation precisely requires high spatial resolution (Fick and Hijmans 2017). Furthermore, different global bioclimatic databases use different methodologies, leading to the poor congruence between them. Thus, using a single database could lead to biased and unreliable predictions, especially in mountainous regions with stronger climatic variances (Morales-Barbero and Vega-Álvarez 2019). There are several global bioclimatic databases, among which only two, i.e., WorldClim ver. 2.1 (Fick and Hijmans 2017) and CHELSA ver. 2.1 (Karger et al. 2017), have high spatial resolution (30 arc-seconds) and recent averages for current BCVs. Therefore, we choose both WorldClim and CHELSA for predicting the habitat distribution of *A. spectabilis*.

WorldClim is the most prominently used global bioclimatic database (Bobrowski et al. 2021a). The latest version of WorldClim (ver. 2.1) is a refined version that includes the spatially interpolated meteorological data from satellites and weather station data. This improved the prediction accuracy for temperature variables; however, other climate variables were only marginally affected (Fick and Hijmans 2017). Climatologies at high resolution for the earth's land surface areas (better known by its acronym CHELSA) offer high-resolution information on BCVs. CHELSA uses statistical downscaling of temperature and precipitation algorithms; additionally, for precipitation, it also incorporates orographic features, thus improving the performance in mountainous regions (Karger et al. 2017).

For climatic data, we choose the standard 19 BCVs released by CHELSA (ver. 2.1) and WorldClim (ver. 2.1). The GeoTIFF files were downloaded for the 19 BCVs under both global bioclimatic databases in 30 arc-second resolution (ca. 1 km²), representing the averaged current climate data for the period 1970–2000 for WorldClim and 1979–2013 for CHELSA (Fick and Hijmans 2017). Using the *Extract by Mask (folder)* tool of SDMtoolbox, the input rasters were clipped using the Uttarakhand shapefile mask and extracted in ASCII format. The ASCII layers were projected to WGS84 projection using the *Define Projection as WGS84 (folder)* tool under SDMtoolbox in ArcGIS. The bioclimatic variables with $r < \pm 0.90$ were retained, and highly correlating variables were omitted using the *Remove Highly Correlated Variables* tool of the SDMtoolbox to avoid any autocorrelations leading to unintentional biasedness. BCVs BIO1, BIO2, BIO3, BIO4, BIO7, BIO12, BIO14, BIO15, BIO17, and BIO18 were the variables for WorldClim after removing correlation, while for CHELSA, the BCVs were BIO1, BIO2, BIO3, BIO7, BIO12, BIO13, and BIO14. Since both the databases had a different set of BCVs so, to prevent any biasedness, we selected the common set of BCVs. Thus, for both databases we used six BCVs (Table 10.1) for habitat distribution modeling, viz., BIO1, BIO2, BIO3, BIO7, BIO12, and BIO14. In addition to the bioclimatic variables, we also used solar radiation (kJ m⁻² day⁻¹) as an additional climatic variable. The data was obtained from WorldClim ver. 2.1 (Fick and Hijmans 2017) at 30 arc-second resolution. The monthly GeoTIFF files were averaged using *Cell Statistics* tool (Spatial Analyst toolbox).

The species of interest occurs in mountainous regions, and the BCVs also use digital elevation models (DEM); therefore, we also used three topographical variables, i.e., elevation, aspect, and slope. The elevation data was obtained from WorldClim ver. 2.1 (Fick and Hijmans 2017) at 30 arc-second resolution. The GeoTIFF elevation raster was projected in WGS84 projection and clipped using Uttarakhand shapefile. The resulting raster was used to compute aspect and slope under the Spatial Analyst toolbox in ArcGIS. A z-factor corresponding to 30 degrees latitude was chosen to calculate the slope raster in degrees.

One edaphic variable, i.e., Global Soil Organic Carbon Map V1.5 released by the Food and Agriculture Organization (FAO), was selected. Soil organic carbon (SOC) being the predominant component of soil organic matter reflects soil quality. SOC is associated with nutrient availability, water retention capacity of the soil, and even structural stability (FAO and ITPS 2018). The GeoTIFF raster was downloaded in

Table 10.1 Environmental variable used for *A. spectabilis* ENM

| Model 1 | |
|---|--|
| BCV codes (units) | Interpretation (scaling factor and offset) |
| CHELSA BIO1 (°C) | Mean annual air temperature (0.1 and - 273.15) |
| CHELSA BIO2 (°C) | Mean diurnal air temperature range (0.1 and 0) |
| CHELSA BIO3 | Isothermality, i.e., BIO2/BIO7 (0.1 and 0) |
| CHELSA BIO7 (°C) | Annual range of air temperature (0.1 and 0) |
| CHELSA BIO12 (kg m ⁻²) | Annual precipitation amount (0.1 and 0) |
| CHELSA BIO14 (kg m ⁻²) | Precipitation amount of the driest month (0.1 and 0) |
| Model 2 | |
| WorldClim BIO1 (°C) | Annual mean temperature |
| WorldClim BIO2 (°C) | Mean diurnal range |
| WorldClim BIO3 (%) | Isothermality, i.e., (BIO2/BIO7) × (100) |
| WorldClim BIO7 (°C) | Temperature annual range |
| WorldClim BIO12 (mm) | Annual precipitation |
| WorldClim BIO14 (mm) | Precipitation of the driest month |
| Variables common to both model 1 and model 2 | |
| Solar radiation (kJ m ⁻² day ⁻¹) | |
| Elevation (meters) | |
| Aspect (degrees) | |
| Slope (degrees) | |
| SOC (Mg ha ⁻¹) | |
| HII | |
| All the environmental variables are at 30 arc-second resolution. For each model there are 12 sets of environmental variables each | |

30 arc-second resolution. It represents SOC for 0–30 cm depth on Mg ha⁻¹ basis (accessed on 16 April 2022 [https://storage.googleapis.com/fao-maps-catalog-data/geonetwork/gsoc/GSOCmap/GSOC map 1.5.0.tif](https://storage.googleapis.com/fao-maps-catalog-data/geonetwork/gsoc/GSOCmap/GSOC%20map%201.5.0.tif)).

For the anthropogenic variable, we choose Global Human Influence Index (HII) version 2 (1995–2004) dataset. The raster data was downloaded at 30 arc-second resolution and obtained from the Socioeconomic Data and Applications Centre (SEDAC) (WCS 2005). HII uses nine datasets broadly grouped into four categories, population density, land transformation, accessibility, and electrical power infrastructure, which describe the human footprint. The index ranges from 0 to 72, with higher scores indicating a higher anthropogenic footprint (Sanderson et al. 2002).

All the environmental layers were masked to the Uttarakhand shapefile, projected in WGS84 projection, and converted to ASCII format using ArcGIS. So, there were a set of 12 environmental variables under each of the two sets, i.e., model 1 and model 2, as indicated in Table 10.1.

10.2.4 Ecological Niche Modeling

ENM is an empirical approach that couples the species occurrences with the environmental predictor variables to model specific environmental constraints relative to the species (species realized niche), which aids in the spatial and temporal mapping of the species habitat distribution (Elith and Franklin 2013). Several species distribution modeling algorithms are based on different principles, and different methodologies exist to use the models. The models could either be stand-alone or in a combination approach (ensemble modeling) which is gaining trend since combining the response from various models improves the prediction accuracy (Kaky et al. 2020). We used a single-model approach and deployed the use of maximum entropy algorithm-based species distribution modeling software MaxEnt (version 3.4.4) (Phillips et al. 2004, 2006, 2017). MaxEnt has been a primary choice for the majority of ENM studies on account of its advantages, viz., it is a presence-only model, works well with both continuous and categorical environmental variables, its regularization parameters avoid over-fitting of the model, flexibility in the choice of threshold selection for binary output, and easy-to-understand distribution results as well as interpretation of environmental variables with habitat suitability (Phillips et al. 2006). Furthermore, the ensemble method requires complex computation, and with limited occurrence records, MaxEnt has proved to be equally robust and accurate in predicting habitat suitability (Kaky et al. 2020); thus, we used MaxEnt for the ENM.

Two sets of MaxEnt models were run, i.e., model 1 and model 2. Model 1 included CHELSA BCVs along with other environmental variables, and model 2 used WorldClim-based BCVs and other environmental variables (Table 10.1). MaxEnt model was executed using auto-feature mode so that MaxEnt automatically decides the best features suited to our dataset. The random test percentage was set to 30%; therefore, 70% of the occurrence records were reserved for training and 30% for testing. We used the entire spatially rarefied occurrence dataset for the maximum use of occurrence records for model building (Phillips et al. 2006). Other settings included checking the check box for creating response curves and Jackknife for testing variable importance (this allows to assign the permutation importance and contribution of each predictor variable), output format was set to logistic threshold for obtaining a binary output, and output file format was chosen as ASCII. Under the Basic Settings tab, the default random seed was selected; regularization multiplier β value was set to 1 (helps to prevent model overcomplexity); background points to default 10,000; and 50 replicates with bootstrap run the method (bootstrap method was chosen due to limited occurrence records). Under the Advance tab, Write Plot Data was selected, maximum iterations were 500, convergence threshold was 0.00001, threshold rule was set to 10-percentile training presence, and under the Experimental tab, Write Background Predictions were selected.

10.2.5 Model Performance and Model Output

We evaluated the performance of both the SDM models, i.e., model 1 (CHELSA BCVs and other variables) and model 2 (WorldClim BCVs and other variables) using threshold-independent techniques since they avoid any issues regarding the selection and influence of threshold values (Fielding and Bell 1997). We used two methods, viz., the area under the receiver operating curve (AUC) and the partial area under the receiver operating curve (pROC), as threshold-independent methods. The AUC score ranges from 0 to 1, with 1 (perfect discrimination) being the greatest predictive ability of the model and 0 showing no predictive ability. Generally, an AUC score from 0.9 to 1.0 is considered excellent, 0.8–0.9 as good, 0.7–0.8 as fair, 0.6–0.7 as poor, and 0.5–0.6 as very poor. At a 0.5 score for presence/background models, no discrimination exists between true and false proportions (random performance) (Swets 1988; Kaky et al. 2020). The AUC scores were obtained from MaxEnt average replicate runs. The pROC considers only the ROC region associated with the data and not the entire AUC range. We also computed the AUC ratio, i.e., the pROC value compared to the null AUC value expected at AUC = 0.5. The AUC ratio value ranges from 0 to 2, with the value of 1 indicating random performance (Peterson et al. 2008; Chaitanya and Meiri 2021). The pROC was calculated using NicheToolBox, an online platform to perform processing steps involved in ecological niche modeling (Osorio-Olvera et al. 2020). For pROC, we used the average ASCII model output from MaxEnt, the proportion of omission was set to 0.05, the random point percentage was set to 50%, and 100 bootstrap iterations were used. We also performed an independent sample t-test on the 100 bootstrap values of the AUC ratio between models 1 and 2 to evaluate the significant difference between the models. Furthermore, the average values of the 12 predictor variables for each of the 50 bootstrap runs were subjected to an independent sample t-test under both models 1 and 2 to determine any significant difference ($p < 0.05$) between the variables.

For both the SDM models, i.e., model 1 and model 2, the average ASCII MaxEnt output file (the result of 50 bootstrap replicates) was converted into raster format using ArcGIS. The average raster suitability files are binary (since a logistic output method was used), with habitat suitability ranging from 0 (unsuitable) to 1 (highly suitable); the value of 1 is generally not achieved. The binary outputs were reclassified into four habitat suitability classes, viz., unsuitable, low, medium, and high suitability. The average 10-percentile training presence (P10) logistic threshold was used to set the lowest limit of habitat suitability above which the suitability classes were classified. The classification was as follows, unsuitable habitat (0–P10 logistic threshold value), low suitability (P10 logistic threshold value–0.4), medium suitability (0.4–0.6), and high suitability (0.6–maximum logistic value). The P10 threshold is a conservative approach, and it considers the habitat suitability of regions lower than the lowest 10% of the training locations to be unsuitable (Di Pasquale et al. 2020). We calculated the total area under each habitat suitability class for both models using *zonal geometry as table* tool under spatial analyst tools in ArcGIS. Furthermore, to determine the percentage distribution of habitat

suitability classes, the final habitat suitability raster file was extracted by mask using each district shapefile for both the models and analyzed for area under each class in each district using *zonal geometry as table* tool in ArcGIS.

10.3 Results

10.3.1 Spatial Autocorrelation of Occurrence Records and Model Performance

There were 26 total occurrence records (Fig. 10.1), of which 14 records showed spatial autocorrelation at >1-km resolution (Fig. 10.3). Therefore, after spatial thinning net 12 occurrence records of *A. spectabilis* were retained, having the least resolution of 1 km so that a grid of environmental variables has at most one occurrence record.

Both the models performed well as per threshold-independent model evaluation parameters AUC and pROC. Model 2 outperformed model 1 in terms of AUC score (Fig. 10.4). Model 1 had a good AUC score; however, model 2 had an excellent score with a very low standard deviation. The mean pROC results also showed model 2 to be the most predictive (Table 10.2). The AUC ratio for model 2 was significantly higher than model 1 [$t(198) = 24.53, p < 0.0001$] (Table 10.2, Fig. 10.5). The difference between the means of AUC for model prediction (AUC partial) and AUC at random was significantly different with $p < 0.001$ for both model 1 and model 2, indicating that both models performed well.

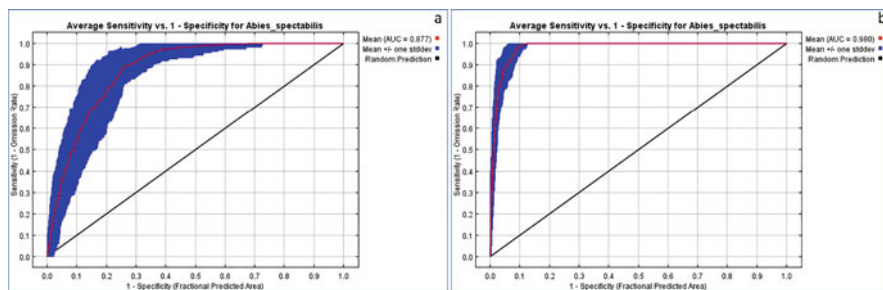


Fig. 10.4 Average area under the receiver operating curves for the two models for *A. spectabilis* with 50 bootstrap runs. (a) AUC for model 1 (notice the greater standard deviation) and (b) AUC for model 2

Table 10.2 *A. spectabilis* model evaluation parameters indicating AUC (MaxEnt, 50 replicate runs), AUC ratio (NicheToolBox, 100 replicate runs), and mean pROC (NicheToolBox, 100 replicate runs). The values indicate the mean with a standard deviation

| Model | AUC | AUC ratio | Mean pROC |
|---------|---------------|--------------|--------------|
| Model 1 | 0.877 ± 0.040 | 1.726 ± 0.09 | 0.863 ± 0.04 |
| Model 2 | 0.980 ± 0.008 | 1.954 ± 0.02 | 0.977 ± 0.01 |

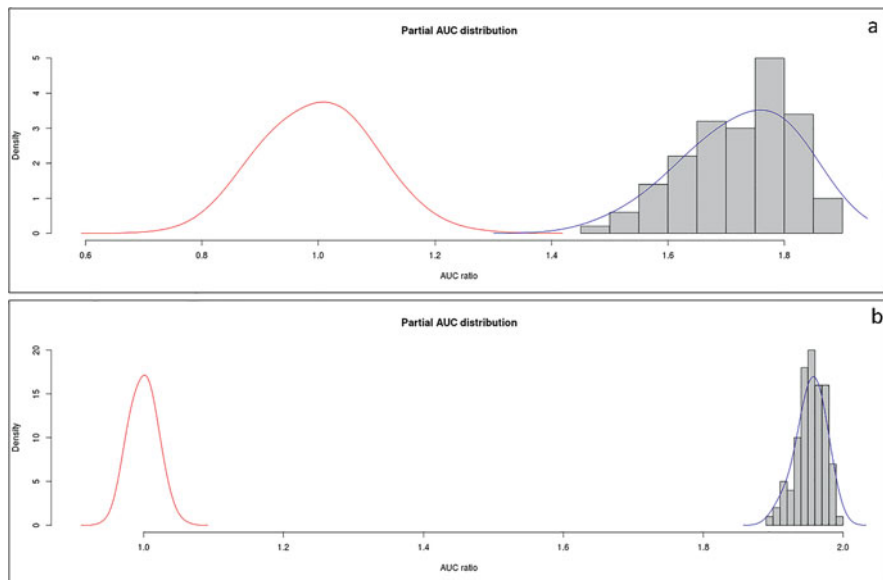


Fig. 10.5 The pROC distribution of *A. spectabilis* under two separate models. (a) pROC distribution under model 1 and (b) pROC distribution under model 2. The shaded bars indicate the frequency distribution of the AUC ratio, and the red-colored bell curve (curve at the left side) indicates the AUC ratios for random models

10.3.2 Influence of Predictor Environmental Variables

The 12 environmental variables chosen under model 1 and model 2 (Table 10.1) had BIO14 as the primary environment variable with the maximum percentage of permutation importance (Fig. 10.6). On a broader overview, the CHELSA BCVs contributed 71.91% of the total permutation importance in model 1, while the WorldClim BCVs contributed 89.43% of the total permutation importance in model 2. For model 1, the top 3 predictor variables based on permutation importance were BIO14 > BIO01 > Soil organic carbon content. For model 2, the trend was BIO14 > Solar radiation > BIO03. In terms of percentage contribution (Fig. 10.6), also BIO14 had the highest contribution among all the environmental variables in both the models.

The Jackknife test for determining variable importance (Fig. 10.7) for models 1 and 2 indicated BIO14 to contain the most useful information and show the highest gain when used in isolation. BIO14 also decreased the maximum gain when omitted, thus indicating that it has information that is not shared by other variables. The result was similar for all three Jackknife tests, i.e., for regularized training gain, test gain, and the AUC.

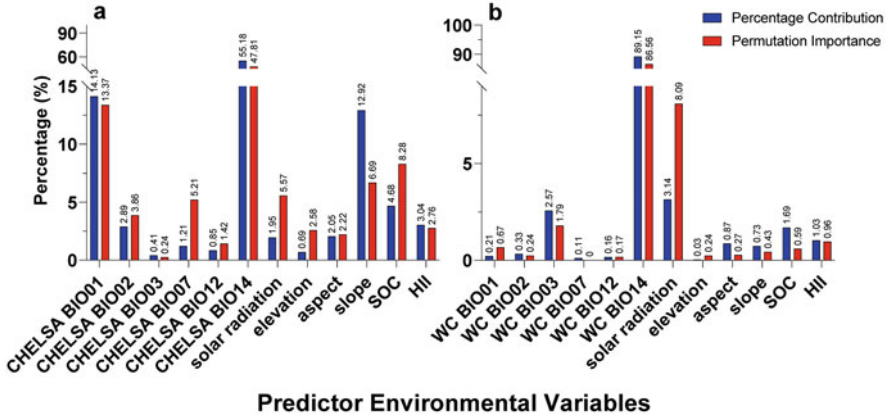


Fig. 10.6 Percentage contribution and permutation importance of the predictor environmental variables for *A. spectabilis*. (a) Predictor variable importance for model 1 and (b) predictor variable importance for model 2

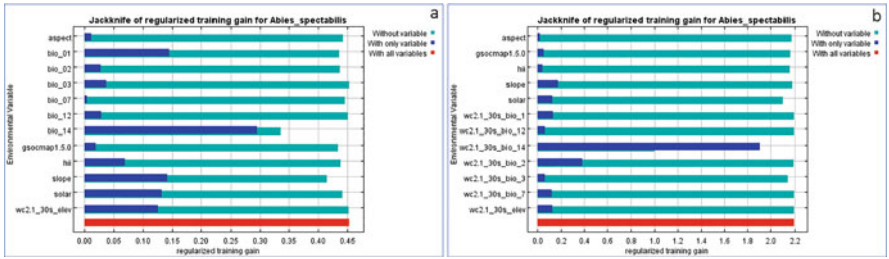


Fig. 10.7 Jackknife test for the regularized training gain for *A. spectabilis*. (a) Model 1 and (b) model 2

10.3.3 Interpretation of the Response Curves

We studied the response curves generated using the particular environmental variable alone to avoid any undue disproportionate impact of variable correlations. Furthermore, we analyzed only the top 3 variables in permutation importance for both models. For model 1, BIO14 and SOC positively influence the habitat distribution of *A. spectabilis*, showing a sigmoid curve, while BIO01 shows a negative influence with an inverse J-shaped curve (Fig. 10.8). On the other hand, in model 2, only BIO14 showed a positive influence on *A. spectabilis* habitat suitability (sigmoid curve), while solar radiation and BIO03 showed a negative trend (Inverse J curve). Model 1 BIO14 ranged from around 5 to 68 kg m⁻² with a habitat suitability of >0.5 at around 29 kg m⁻². BIO01, on the other hand, declined with a suitability of >0.5 at ca. 4.35 °C. SOC showed a positive trend with values ranging from ca. 17 to 67 t ha⁻¹ and a suitability of >0.5 at ca. 42.5 t ha⁻¹. Under model 2, BIO14 ranged from ca. 10 to 38 mm with a suitability of >0.5 at ca. 31 mm. Solar

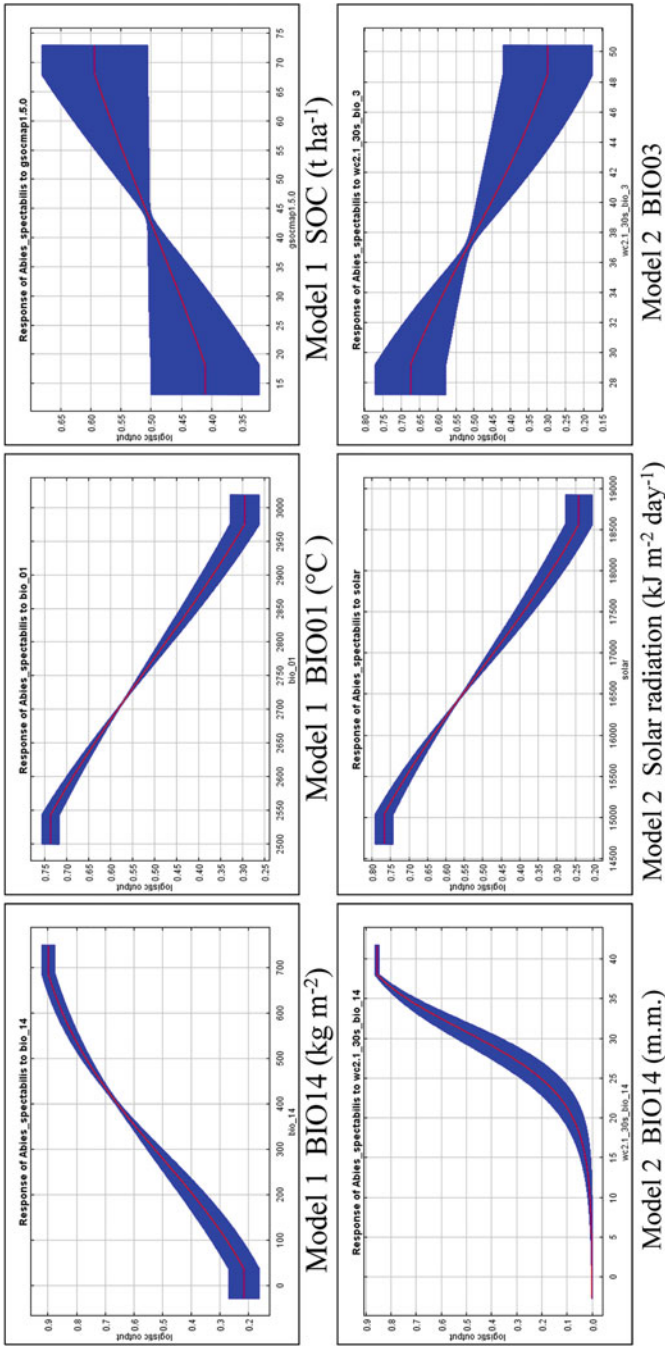


Fig. 10.8 Response curves of *Abies spectabilis* to environmental variables. X-axis represents the value of the environment variable, while the Y-axis represents the logistic value of habitat suitability. The red line represents the mean of MaxEnt runs, while the blue region represents the standard deviation

Table 10.3 Average values of 50 replicate runs of each predictor variable for the occurrence records

| Environmental variable | Model 1 ^a | Model 2 |
|---|----------------------|------------------|
| BIO1 (°C) | 3.64 ± 0.88 | 6.54 ± 0.77 |
| BIO2 (°C) | 10.25 ± 0.28 | 9.55 ± 0.18 |
| BIO3 (%) | 36.36 ± 0.86 | 37.68 ± 0.65 |
| BIO7 (°C) | 28.20 ± 0.51 | 25.38 ± 0.51 |
| BIO12 (mm) | 2770.57 ± 165.49 | 1699.51 ± 60.84 |
| Bio14 (mm) | 30.56 ± 2.58 | 31.84 ± 1.28 |
| Solar radiation (kJ m ⁻² day ⁻¹) | 16758.33 ± 44.72 | 16782.96 ± 57.64 |
| Elevation (meters) | 3236.10 ± 89.30 | 3217.14 ± 108.73 |
| Aspect (degrees) | 170.23 ± 32.16 | 165.12 ± 34.68 |
| Slope (degrees) | 17.80 ± 2.75 | 18.55 ± 2.84 |
| SOC (t ha ⁻¹) | 43.16 ± 1.99 | 44.20 ± 2.72 |
| HII | 15.62 ± 1.57 | 16.49 ± 1.69 |

^aThe values for CHELSA BCVs (model 1) are corrected for scale and offset

radiation declined the habitat suitability with a suitability of >0.5 at ca. 16800 kJ m⁻² day⁻¹. BIO03 also showed a similar trend as solar radiation with a suitability of >0.5 at ca. 38% (Fig. 10.8).

The values of the 12 environmental predictor variables over the species occurrence points were obtained from MaxEnt sample average files for each of the 50 replicates under both models 1 and 2 (Table 10.3). Only elevation, slope, and aspect did not have any statistically significant difference between the means ($p > 0.05$) as determined using an independent sample t-test, rest all the pairs between models 1 and 2 showed statistically significant difference ($p < 0.05$).

10.3.4 Current Habitat Suitability of *A. spectabilis*

The average P10 training presence logistic threshold values were 0.3784 and 0.2724 for models 1 and 2. These values were regarded as the threshold for suitability cutoff, and based on this, the current habitat suitability map was drafted (Fig. 10.9). Model 1 had the highest percentage distribution for all three suitability classes compared to model 2 (Table 10.4). Both the models showed a statistically significant strong positive correlation in their percentage distribution of habitat suitability classes indicating similar predictions trend ($r = 0.966$, $n = 4$, $p = 0.034$). *A. spectabilis* habitat suitability area in the Indian Central Himalaya as per model 1 was 16,324.57 km², while for model 2, it was 3323.86 km².

The spread of habitat suitability of *A. spectabilis* is toward the northern region of Uttarakhand, having more prominence of higher elevation (Fig. 10.1). The majority of the unsuitable and low suitable habitat suitability regions were situated in the southern part of the state (Fig. 10.9). The niche overlap map (Fig. 10.11) shows model 1 to predict higher suitable regions than model 2. Moreover, the overlap also

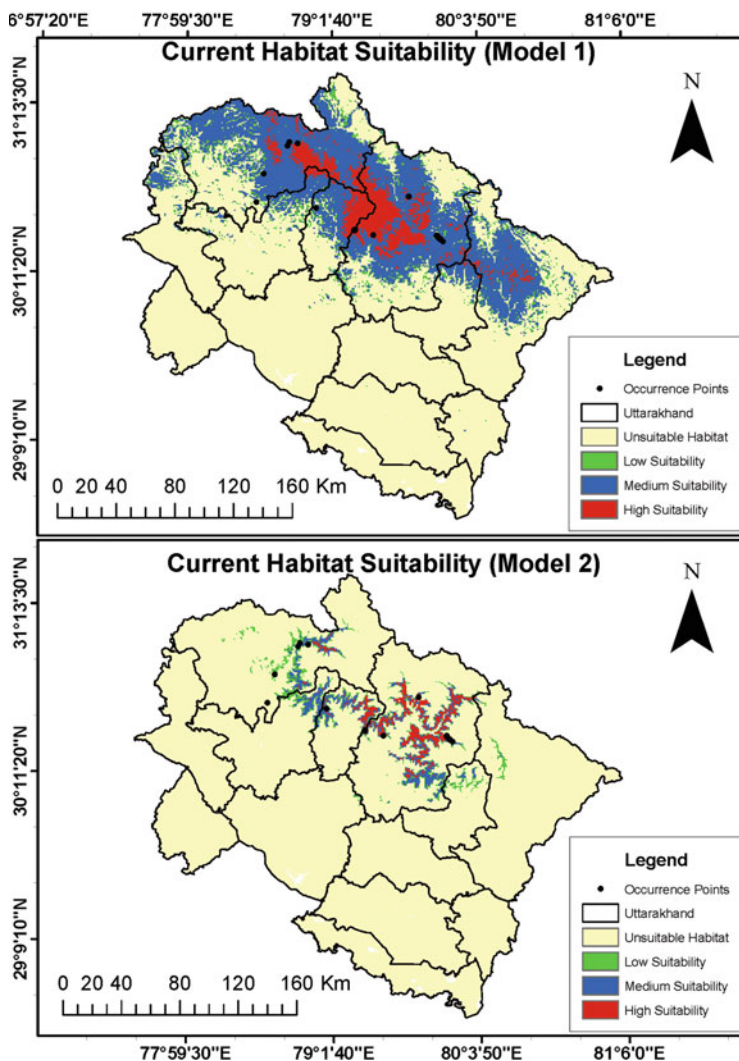


Fig. 10.9 Current habitat suitability map of *A. spectabilis* in the Indian Central Himalaya under models 1 (top) and 2 (bottom). The unsuitable class has the 10-percentile training presence average logistic threshold value as cutoff

shows that the region predicted as suitable by only model 2, excluding the overlap areas, was smaller than model 1. Haridwar and Udham Singh Nagar were the only two districts showing complete *A. spectabilis* habitat unsuitability as per model 1; however, model 2 predicted Almora, Champawat, Dehradun, and Nainital to be unsuitable in addition to Haridwar and Udham Singh Nagar. For model 1, the districts with the highest suitability region were Rudraprayag (19.55%) > Chamoli (16.72%) > Uttarkashi (8.25%), while for model 2 the trend was Chamoli

Table 10.4 Current habitat suitable area (km²) of *A. spectabilis* under different suitability classes in both models 1 and 2. Values in parenthesis indicate the percentage of the total land area (53,483 km²) of Uttarakhand

| Habitat suitability class | Model 1 | Model 2 |
|---------------------------|------------------|------------------|
| Unsuitable | 37158.43 (69.48) | 50159.14 (93.79) |
| Low suitability | 2127.15 (3.98) | 1222.03 (2.28) |
| Medium suitability | 11561.03 (21.62) | 1274.97 (2.38) |
| High suitability | 2636.39 (4.93) | 826.86 (1.55) |

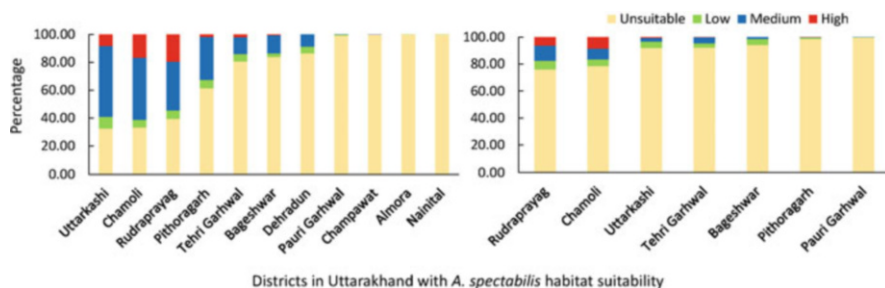


Fig. 10.10 Habitat suitability percentage of *A. spectabilis* in each district of Uttarakhand state under model 1 (left stacked column) and model 2 (right stacked column graph). Districts with 100% region as unsuitable *A. spectabilis* habitat were omitted

(8.43%) > Rudraprayag (6.20%) > Uttarkashi (0.53%). Uttarkashi (50.86%) had the highest percentage of medium habitat suitability in model 1, while Rudraprayag (11.35%) in model 2. Uttarkashi district also had the highest proportion of low habitat suitable region (8.36%) in model 1 and Rudraprayag (6.32%) in model 2 among all the 13 districts of Uttarakhand (Fig. 10.10).

10.4 Discussion

10.4.1 Species Occurrence Records and the Performance of Models

Occurrence records following spatial thinning (Fig. 10.3) for this study were relatively low (12 points). This is because *A. spectabilis* occurs in high-elevation zones in the Himalayas (Fig. 10.1) prominently in rugged and inaccessible terrains, thus making field surveys difficult. Low occurrence points are not unusual in literature; for instance, Kumar and Stohlgren (2009) used 11 occurrence records (the only known occurrence) to predict the habitat distribution of a threatened and endangered tree species *Canacomyrca monticola* Guillaumin. *A. spectabilis* is a treeline coniferous species (Fig. 10.2) that is endemic to the Himalayas and occurs in a narrow elevation zone generally spanning from 3000 to 4000 m.a.s.l. (Zhang et al. 2011). The vegetation pattern in the Indian Central Himalayas along the elevational

gradient shows fairly consistent sub-alpine vegetation with selected species that can withstand harsh environmental conditions (Singh and Singh 1987; Sharma et al. 2018; Tiwari et al. 2018). Such species, including *A. spectabilis*, have a specialized niche; modeling such species even with lower occurrence records is much easier since the species with broader geographical distribution require a more significant number of occurrence records for higher model accuracy. Hernandez et al. (2006) experimentally showed that models run using occurrence points as low as 10 generated almost similar results as those run with twice the size predominantly for the species with the specialized niche. They also supported that the MaxEnt model performs the strongest even with low occurrence records on its regularization parameters. Our occurrence records (26 records) were, however, lower as compared with the records used for habitat suitability prediction of *A. spectabilis* in Nepal (94 records) (Chhetri et al. 2018). We also recommend including true absence points in the modeling of the habitat distribution of treeline species since certain environmental factors limit the spread of these species beyond the treeline. Encoding these factors in the modeling parameters will yield greater accuracy in habitat suitability prediction, especially for future habitat modeling studies under different climate change scenarios.

The predictive performance of the models was tested using three parameters, viz., AUC, pROC, and AUC ratio (Table 10.2). This method is advantageous since error and bias associated with selecting the threshold value are omitted; furthermore, different models would have different threshold cutoffs making model comparison problematic (Phillips et al. 2006). Model 2 outperformed model 1 (Table 10.2, Figs. 10.4 and 10.5) in all three model testing parameters; however, model 1 was only marginally lower than model 2, suggesting the successful habitat prediction from both models. AUC was not used as the only model evaluation statistic as the error components are weighted equally. Moreover, comparison with AUC becomes problematic since the commission errors are calculated along with the entire range (0–1) even though the predicted occurrence may not span that range; therefore, we used pROC and AUC ratio (Table 10.2, Fig. 10.5) which helps overcome these issues (Peterson et al. 2008).

Chhetri et al. (2018) reported a high AUC value (AUC = 0.89) for *A. spectabilis* habitat distribution in Nepalese Himalaya. High mean AUC values were also reported for *Picrorhiza kurroa* Royle ex Benth. (AUC = 0.915) (Rawat et al. 2022) and *Dactylorhiza hatagirea* (D. Don) Soó (AUC = 0.868) (Chandra et al. 2021); the two endangered alpine medicinal plants in Uttarakhand having similar to higher elevational range as *A. spectabilis*. *Q. semecarpifolia* (AUC = 0.982), a broadleaf treeline oak species in the Indian Central Himalaya, also showed excellent AUC value (Chakraborty et al. 2016). We do not intend to compare our AUC values with these studies but only show a near comparable range for the model prediction of these species, which occur in the same niche space as *A. spectabilis*. The comparison of AUC between different species, across different regions and using varying modeling parameters, is not valid due to the differences in the potential distribution area. However, AUC could be used to compare two environmental datasets (Fig. 10.4), provided the species and area of interest remain the same (Peterson et al. 2011).

10.4.2 Use of Two Global Bioclimatic Databases

There are only two predominant high-resolution bioclimatic databases, i.e., WorldClim and CHELSA, which differ in their BCV prediction algorithm. WorldClim uses a spatial interpolation of climate data, and this technique is considered less ideal than the statistical downscaling method used by CHELSA. The spatial interpolation methods usually perform less optimally in regions with uneven topography, like mountains. Furthermore, in extreme environments like treeline ecotone or alpine regions, the environmental features have a predominant say in shaping the habitat distribution of the species (Morales-Barbero and Vega-Álvarez 2019). All the bioclimatic variables are based upon two primary datasets temperature and precipitation. While both CHELSA and WorldClim showed congruence for temperature predictors, the prediction accuracy for CHELSA precipitation pattern is more sensitive in the mountainous regions than WorldClim due to the incorporation of orographic features (Karger et al. 2017).

Furthermore, Bobrowski and Schickhoff (2017) evaluated the efficacy of global climate datasets in modeling the habitat distribution of a principal Himalayan treeline broadleaf species, *B. utilis*. They concluded CHELSA to show greater accuracy with predictions closer to actual field observations. They also found WorldClim to over-predicting the habitat distribution and thus cautioned against the use of WorldClim BCVs alone in the Himalayan landscape without scrutinizing. Therefore, we used both WorldClim- and CHELSA-based BCVs for the ENM of *A. spectabilis*. In a recent critical review on ENM, Bobrowski et al. (2021b) reported that there are only three studies in the Himalayas that used both WorldClim- and CHELSA-based BCVs to compare the modeling performance. Therefore, our study adds to the performance of the two global bioclimatic databases and their limited knowledge of the Himalayan landscape.

Furthermore, our study is probably the first to use a comparative approach to the ENM of the endemic Himalayan treeline conifer *A. spectabilis*. With model 2 having outperformed model 1 on model validation parameters, we infer that in our study, WorldClim-based BCVs (model 2) performed much better than CHELSA (model 1). The performance of CHELSA was only marginally lower, and thus we do not discriminate against its use. However, we recommend further improving the model by adding more occurrence points and including true species absence points for greater validation and accuracy.

10.4.3 Predictor Environmental Variables and their Response Curves

We focused on the permutation importance rather than percentage contribution in deciding the importance of environmental variables since the percentage contribution depends upon the path MaxEnt chosen to build the optimal model. The contribution would vary with each run due to the change in the modeling algorithm. Furthermore, we also used the Jackknife test, wherein the model was run multiple times. Each variable was first modeled alone, excluding it and including the

remaining variables to interpret the degree of gain or loss for that parameter (Phillips 2017). Interestingly, models 1 and 2 had the precipitation of the driest month (BIO14) as the most influential predictor environmental variable having the highest permutation importance and percentage contribution (Fig. 10.6). Even from the Jackknife test (Fig. 10.7), BIO14 had the highest gain when used in isolation and caused the most loss in gain when omitted under both models 1 and 2, thus confirming it to be the most influential predictor variable of *A. spectabilis* in Uttarakhand. In Uttarakhand Himalaya, BIO14 was also deemed to be the most significant predictor variable for the habitat distribution of Himalayan endangered medicinal herb *P. kurroa* (Rawat et al. 2022), critically endangered medicinal plant *Lilium polyphyllum* D.Don (Dhyani et al. 2021), and multipurpose shrub species *Hippophae salicifolia* D.Don (Dhyani et al. 2018). In other parts of the IHR and similar elevational range, species like *Rheum webbianum* Royle, a vulnerable medicinal herb in northwest Himalaya, had BIO14 as the most important predictor variable (Wani et al. 2021). All the aforementioned plant species have a similar to higher elevational range as *A. spectabilis*; moreover, *P. kurroa*, *H. salicifolia*, and *R. webbianum* are also found in Tungnath region having *A. spectabilis* treeline ecotone (Rai et al. 2012b). The trend, however, is not universal, and *D. hatagirea*, a threatened medicinal orchid that also occurs in the Tungnath region along the *A. spectabilis* treeline (Rai et al. 2012b), showed a mean diurnal range (BIO2) as the most significant predictor variable with the highest permutation importance for its ENM in Uttarakhand (Chandra et al. 2021). Thus, the species occurring in similar habitats do not always share similar niche requirements. Chhetri et al. (2018) critically modeled the habitat distribution of prominent treeline species in the Nepalese Himalaya and found elevation as the strongest predictor variable for *A. spectabilis* followed by isothermality (BIO3) in their model using 94 occurrence records for *A. spectabilis* alone.

Our results indicate that *A. spectabilis* is sensitive to dry seasons and constantly requires a minimum moist climate for habitat suitability. Moreover, BIO14 for both model 1 and model 2 showed a sigmoidal response curve (Fig. 10.8), indicating a positive relationship between precipitations in the driest month with predicted suitability. We also observed that the average value for BIO14 under the occurrence records (Table 10.3) for both models was well within the response curve range for BIO14 (Fig. 10.8) and since the average current value is around 30 mm for both the models thus as per the response curve higher values will lead to more habitat suitability for *A. spectabilis*. The value for the precipitation of the driest month reflects the bare minimum amount of precipitation required for the habitat suitability in Uttarakhand region, since November is the month that usually receives the least annual rainfall (Climate-Data.org 2022). Therefore, the precipitation during this month predominantly characterizes the *A. spectabilis* habitat suitability. Singh and Negi (2018), in their phenological studies of Central Himalayan treeline species, showed October–November months as the seed maturation duration for *A. spectabilis*. Therefore, this period is critical since precipitation ensures the establishment of seed set and further seed germination. Singh et al. (2018) indicated the importance of winter temperatures, especially November and February months,

in regulating the growth (radial growth) of *A. spectabilis* in the Tungnath region of Uttarakhand. Additionally, they predicted the winter warming trend to be a probable cause for the loss of regeneration for *A. spectabilis*. Our results confirm this observation since BIO1 (annual mean temperature) was the second most important predictor variable under model 1 (Fig. 10.6), which showed an inverse J trend (Fig. 10.8), inferring habitat loss with increasing warming. Solar radiation was the second most important predictor variable in model 2 which also showed a negative trend, thus indicating increasing levels of solar radiation detrimental to habitat suitability. Globally the levels of solar radiation have been studied either as a key factor (Bader et al. 2007) or as one of the factors (Barbeito et al. 2012) responsible for the alpine treeline formation, regeneration, and mortality. The third environmental variable having the highest permutation importance (Fig. 10.6) for both models 1 (SOC) and 2 (BIO3) had a high standard deviation, and the permutation importance was less than 5%. An inverse J relationship of isothermality (BIO3) with habitat suitability (Fig. 10.8) indicates that *A. spectabilis* has a narrow range to tolerate the temperature oscillations between monthly temperature range and annual temperature range, thus indicating its narrow niche requirements for its habitat suitability. BIO3 was found to be the most important BCV for three prominent alpine treeline species *A. spectabilis*, *B. utilis*, and *P. wallichiana* in the Nepal Himalaya (Chhetri et al. 2018). The importance of SOC as a predictor variable indicates the contribution of edaphic factors in regulating habitat suitability. Higher SOC values are associated with increased nutrient availability in soil on account of increased microbial and enzymatic activity in soil (Siwach et al. 2021). Moreover, the sigmoidal response curve obtained (Fig. 10.8) infers the positive association of increasing soil carbon stock with habitat suitability.

However, one significant concern is regarding the selection of the environmental variables. Since each study has either difference in study species or study region, and even if these components are similar, there would be a difference in occurrence records. This would cause differential autocorrelation in the BCVs, thus resulting in a heterogeneous selection of BCVs. Furthermore, the variables omitted to reduce spatial autocorrelation might show significant importance for the same species in different regions. Therefore, the selected predictor variables must be used cautiously. Similar concerns were also reflected by others (Kumar 2012; Chhetri et al. 2018; Yoon and Lee 2021).

10.4.4 Current Habitat Suitability of *A. spectabilis*

The strong correlation found between the habitat suitability classes for models 1 and 2 indicates similar trend prediction by both models. The suitability area under medium suitability (0.4–0.6) is much higher than low suitability (P10 threshold–0.4) since the threshold value is quite large (larger than 0.2), thereby making the size of the low suitability class smaller. The suitable area predicted by model 1 was around five times greater than model 2 (Table 10.4). Surprisingly the average values for the occurrence locations for all the environmental predictor variables

(Table 10.3) were only marginally different; still, the output predictions turned out to be substantially diverse. We attribute this difference solely to the two global bioclimatic databases used since the other environmental variables were similar under both models. In this study, BIO14 was the most important predictor variable under both models, and this variable is derived from annual precipitation values. Since precipitation-related CHELSA BCVs have been deemed more accurate due to the edge of statistical downscaling approach over spatial interpolation of WorldClim (Karger et al. 2017) therefore, CHELSA-based model 1 might have predicted a larger area. Bobrowski and Schickhoff (2017) highlighted a critical note about the distribution of weather stations in the Himalayas; not only their number is scarce, but also they are heterogeneously distributed along the Himalayan range. Moreover, those present have an almost negligible presence in the treeline elevations due to inaccessible terrain, poor connectivity, and harsh weather conditions. This makes the BCV data for higher elevations more susceptible to errors. Furthermore, due to complex topographical terrain such as slope degrees, slope aspect, windward and leeward side, etc., local site-specific weather patterns develop that modulate the habitat suitability of vegetation on a local scale. In our opinion, the global bioclimatic database that captures the maximum amount of this fine variability would yield the most accurate prediction. Though both the models performed equally well, model 2 with WorldClim BCVs performed slightly better. Therefore, we believe that the current habitat distribution from model 2 has greater accuracy.

Interestingly, the districts with high habitat suitability class (0.6–maximum value) for models 1 and 2 were the same (Fig. 10.9). This infers that *A. spectabilis* is chiefly distributed in Rudraprayag, Chamoli, and Uttarkashi districts. This is also evident from the overlay map, wherein the maximum overlay is primarily situated in these three districts (Fig. 10.11). The primary region is confined to the eastern part of Uttarkashi, the northern region of Tehri Garhwal, the northern part of Rudraprayag, central to the northern fringes of Chamoli, and the western part of Pithoragarh and northern region of Bageshwar district (Fig. 10.11). These regions have the appropriate cold sub-alpine climate and appropriate mesic conditions. Our predicted regions for *A. spectabilis* were similar to the model predictions for *B. utilis* (Singh et al. 2013) and *D. hatagirea* in Uttarakhand (Chandra et al. 2021). These species share their elevational range with *A. spectabilis*. Overall, the highly suitable regions of the species are distributed in a tight group toward the northern region of Uttarakhand. The absence in the western portion of Uttarkashi district could be due to reduced annual precipitation in the district from east to west direction; furthermore lower suitability in the east (eastern portion of Pithoragarh) is due to reduced early winter season precipitation (November) (Singh and Singh 1987) which is critical for *A. spectabilis* as per our model predictions.

10.4.5 Implications for Conservation and Future Prospects

Being a near-threatened species, the conservation of *A. spectabilis* demands priority. From our current habitat suitability map (Fig. 10.9) and the area under different

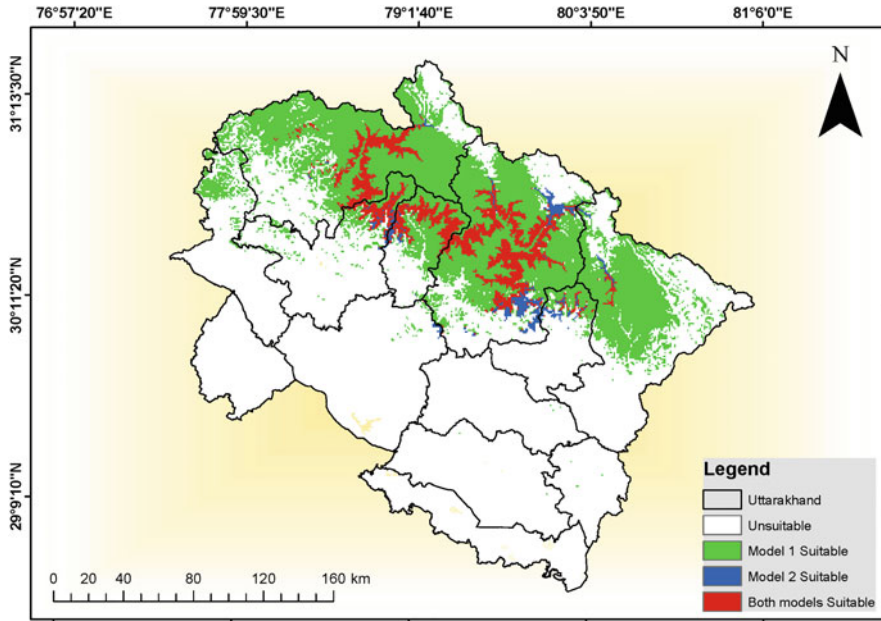


Fig. 10.11 An overlay of model 1 and model 2 habitat suitability regions for current habitat distribution of *A. spectabilis* in Uttarakhand. The poinsettia red color indicates the regions suitable under models 1 and 2

habitat suitability classes (Table 10.4), these ranges are higher than the actual occurrence of the species. This is because the MaxEnt-based habitat suitability model indicates the regions with environmental conditions suitable for *A. spectabilis*, i.e., the fundamental niche. However, the true distribution of the species is restricted by several factors such as geographic barriers, anthropogenic disturbances, and even biotic pressure (Phillips et al. 2006). These factors shape the actual distribution of the species, thus marking its realized niche. Therefore, policy planners must be cautious in using habitat suitability predictions. The regions we suggest as highly suitable or suitable represent the regions with environmental conditions conducive to *A. spectabilis*. They may or may not show their actual occurrence in those locations. However, being suitable, these regions could be selected for raising assisted regeneration and plantations of *A. spectabilis* for conservation. Furthermore, planners must have *A. spectabilis* as the primary choice for plantations in these regions.

Uttarkashi, Rudraprayag, and Chamoli are the predominant districts with high to medium habitat suitability (Fig. 10.10). Most of the highly suitable habitat regions in Uttarkashi district and the regions common to models 1 and 2 from the overlay map (Fig. 10.11) lie in the Gangotri National Park region. For Rudraprayag also, the suitable habitat falls under Kedarnath Wildlife Sanctuary. However, for Chamoli district, the eastern region is in the protected area status under Kedarnath Wildlife

Sanctuary, while the western region falls under Nanda Devi biosphere reserve; however, the central portion does not lie in any protected area category. Therefore, focusing on this region is critical since, under models 1 and 2, this region has a prominent presence of highly suitable habitat for *A. spectabilis*. Apart from these districts, the upper fringe of Tehri Garhwal, Bageshwar, and the northwestern portion of Pithoragarh also have noticeable regions with high suitability for *A. spectabilis*. Such areas should be physically monitored to assess the species' presence and its regeneration status which must be enhanced for future habitat security.

Those regions which are under the protected area must also not be considered entirely conserved. For instance, in our earlier work (Kaushal et al. 2021) in the *A. spectabilis*-dominant forest at Tungnath, Uttarakhand, we found the forest to show unimodal girth class distribution with negligible occurrence in the 10–20-cm diameter at breast height (DBH) range indicating poor regeneration. Furthermore, the region has immense grazing pressure, especially from nomadic grazers, and intense fuelwood demand from the local community, especially during the pilgrim and tourist season (Rai et al. 2012a). Stringent monitoring is essential, especially in the protected areas, though understandably, the livelihood of the local communities is dependent upon the surrounding natural resources, and the growing tourist pressure over the years has led to extensive utilization beyond the sustainable capacity. Specified regions should be demarcated for grazing, and using species with efficient regeneration for fuelwood could help reduce the anthropogenic pressure on this endemic Himalayan conifer. Our observations show that many threatened medicinal plants have similar niche requirements as *A. spectabilis*. Therefore, it is a win-win strategy where the conservation of one species would also ensure the conservation of several associated species. Thus, preserving the present habitat and using our predictions for suitable regions for expanding the habitat using *A. spectabilis*-assisted regeneration and plantation are the optimum management requirements.

In terms of future perspectives, we suggest an extensive hyper-accurate survey for delineating the occurrence records of *A. spectabilis* throughout the state. Being a treeline species determining absence points near the treeline would also help fine-tune the models for future climate predictions to accurately monitor the species shift under changing climate scenarios. Presently, we omitted majority of the BCVs on account of autocorrelation, and determination of actual predictor variables associated with the species in the future would help increase the accuracy of predictions. We avoided future climate modeling that can be taken after such issues are addressed to determine the geographical regions with the most significant habitat loss.

10.5 Conclusions

The accuracy of the habitat suitability model is as good as the input parameters. The results indicate model 2 to have greater predictive power; however, the performance of model 1 was also not poor. This methodological dilemma can be avoided by

selecting the highly suitable regions under both models since CHELSA-based BCVs are more accurate with precipitation-based BCVs, and for our study the most important predictor variable was the precipitation amount in the driest month (BIO14). The information from the most important predictor environment variables must be associated with conservation planning approaches especially in plantations wherein the conditions can be modulated for *A. spectabilis* suitability. The species has mere 1.55% area as highly suitable (model 2) in Uttarakhand, and this region is further tightly grouped into five northern districts, i.e., Uttarkashi, Tehri Garhwal, Rudrapur, Chamoli, and Pithoragarh. Though a few of these districts have protected areas that encompass the high suitability regions, our opinion is that for efficient management, the high-elevation sub-alpine to alpine regions for all these northern districts must be under a common protected area status. This would help conserve *A. spectabilis* along with other endangered species that have a similar ecological niche. The regions with current occurrence reflect the realized niche space of *A. spectabilis* and require proactive monitoring. The conservation in these regions would only be possible with the complete support of the local stakeholders and their inclusion in the conservation planning processes. This is critical since the habitat suitability of *A. spectabilis* is at high-elevation regions where regular monitoring can become problematic; in such situation making the local people aware of the conservation necessity would help the situation. The present condition of *A. spectabilis* is perilous, and without any conservation response, the situation can become much worse since this species is one of the dominant forest-forming species in high-elevation alpine timberline – treeline ecotone. Therefore, assisted regeneration, expanding habitat by plantations in the predicted suitable regions, and conservation of the current population are prudent.

Acknowledgments The authors acknowledge the Principal Chief Conservator of Forest (Chief Wildlife Warden), Uttarakhand, and DFO, Kedarnath Wildlife Sanctuary, for their necessary research permission and logistic support during the research. The corresponding author acknowledges the financial support received from the Science and Engineering Research Board (SERB), Government of India, through research project no. EEQ/2016/000164, and Institution of Eminence, University of Delhi (IoE/2021/12/FRP), Faculty Research Programme (FRP), sanctioned during 2021–2022 and 2022–2023. The first author thanks the University Grants Commission (UGC), New Delhi, for providing Senior Research Fellowship. Anshu Siwach thanks the Council of Scientific and Industrial Research, New Delhi, for providing financial assistance as Junior Research Fellowship. Prachi Sharma thanks the UGC and the University of Delhi for the non-NET fellowship.

References

- Adhikari D, Tiwary R, Singh PP, Upadhaya K, Singh B, Haridasan KE, Bhatt BB, Chettri A, Barik SK (2019) Ecological niche modeling as a cumulative environmental impact assessment tool for biodiversity assessment and conservation planning: a case study of critically endangered plant *Lagerstroemia minuticarpa* in the Indian Eastern Himalaya. *J Environ Manag* 243:299–307. <https://doi.org/10.1016/j.jenvman.2019.05.036>

- Allen MR, Dube OP, Solecki WA, Aragón-Durand F, Cramer W, Humphreys S, Kainuma M, Kala J, Mahowald N, Mulugetta Y, Perez R, Wairiu M, Zickfeld K (2019) Framing and context. In: Masson-Delmotte V, Zhai P, Portner H-O, Roberts D, Skea J, Shukla PR, Pirani A, Moufouma-Okia W, Péan C, Pidcock R, Connors S, Matthews JBR, Chen Y, Zhou X, Gomis MI, Lonnoy E, Maycock T, Tignor M, Waterfield T (eds) Global warming of 1.5°C. An IPCC special report on the impacts of global warming of 1.5°C above pre-industrial levels and related global greenhouse gas emission pathways, in the context of strengthening the global response to the threat of climate change. Intergovernmental Panel on Climate Change (IPCC), Geneva, p 84
- Attri SD, Chug S (2021) Annual Report 2020. Information Science & Knowledge Resource Development Division, Indian Meteorology Department, New Delhi
- Attri SD, Tyagi A (2010) Climate profile of India. Environment Monitoring and Research Center, India Meteorology Department, New Delhi
- Bader MY, van Geloof I, Rietkerk M (2007) High solar radiation hinders tree regeneration above the alpine treeline in northern Ecuador. *Plant Ecol* 191(1):33–45. <https://doi.org/10.1007/s11258-006-9212-6>
- Barbeito I, Dawes MA, Rixen C, Senn J, Bebi P (2012) Factors driving mortality and growth at treeline: a 30-year experiment of 92 000 conifers. *Ecology* 93(2):389–401. <https://doi.org/10.1890/11-0384.1>
- Becker A, Bugmann H (eds) (2001) Global change and mountain regions. The mountain research initiative. IGBP Report 49, Stockholm
- Beniston M (2003) Climatic change in mountain regions: a review of possible impacts. *Climate Change* 59:5–31. <https://doi.org/10.1023/A:1024458411589>
- Bhutiyan MR (2015) Climate change in the Northwestern Himalayas. In: Joshi R et al (eds) Dynamics of climate change and water resources of Northwestern Himalaya. Springer, Cham, pp 85–96
- Bobrowski M, Schickhoff U (2017) Why input matters: selection of climate data sets for modelling the potential distribution of a treeline species in the Himalayan region. *Ecol Model* 359:92–102. <https://doi.org/10.1016/j.ecolmodel.2017.05.021>
- Bobrowski M, Weidinger J, Schickhoff U (2021a) Is new always better? Frontiers in global climate datasets for modeling treeline species in the Himalayas. *Atmos* 12(5):543. <https://doi.org/10.3390/atmos12050543>
- Bobrowski M, Weidinger J, Schwab N, Schickhoff U (2021b) Searching for ecology in species distribution models in the Himalayas. *Ecol Model* 458:109693. <https://doi.org/10.1016/j.ecolmodel.2021.109693>
- Brown JL, Bennett JR, French CM (2017) SDMtoolbox 2.0: the next generation Python-based GIS toolkit for landscape genetic, biogeographic and species distribution model analyses. *PeerJ* 5:e4095. <https://doi.org/10.7717/peerj.4095>
- Chaitanya R, Meiri S (2021) Can't see the wood for the trees? Canopy physiognomy influences the distribution of peninsular Indian Flying lizards. *J Biogeogr* 49(1):1–13. <https://doi.org/10.1111/jbi.14298>
- Chakraborty A, Joshi PK, Sachdeva K (2016) Predicting distribution of major forest tree species to potential impacts of climate change in the central Himalayan region. *Ecol Eng* 97:593–609. <https://doi.org/10.1016/j.ecoleng.2016.10.006>
- Chandra N, Singh G, Lingwal S, Jalal JS, Bisht MS, Pal V, Bisht MPS, Rawat B, Tiwari LM (2021) Ecological niche modeling and status of threatened alpine medicinal plant *Dactylorhiza hatagirea* D. Don in Western Himalaya. *J Sustain For*:1–17. <https://doi.org/10.1080/10549811.2021.1923530>
- Chhetri PK, Gaddis KD, Cairns DM (2018) Predicting the suitable habitat of treeline species in the Nepalese Himalayas under climate change. *Mt Res Dev* 38(2):153–163. <https://doi.org/10.1659/MRD-JOURNAL-D-17-00071.1>
- Chitale V, Behera MD (2019) How will forest fires impact the distribution of endemic plants in the Himalayan biodiversity hotspot? *Biodivers Conserv* 28:2259–2273. <https://doi.org/10.1007/s10531-019-01733-8>

- Climate-Data.org (2022) Climate data for cities worldwide. <https://en.climate-data.org/asia/india/uttarakhand-763/>. Accessed 20 Apr 2022
- Dhyani S, Kadaverugu R, Dhyani D, Verma P, Pujari P (2018) Predicting impacts of climate variability on habitats of *Hippophae salicifolia* (D. Don) (Seabuckthorn) in Central Himalayas: future challenges. *Eco Inform* 48:135–146. <https://doi.org/10.1016/j.ecoinf.2018.09.003>
- Dhyani S, Kadaverugu R, Pujari P (2020) Predicting impacts of climate variability on Banj oak (*Quercus leucotrichophora* A. Camus) forests: understanding future implications for Central Himalayas. *Reg Environ Chang* 20(4):1–13. <https://doi.org/10.1007/s10113-020-01696-5>
- Dhyani A, Kadaverugu R, Nautiyal BP, Nautiyal MC (2021) Predicting the potential distribution of a critically endangered medicinal plant *Lilium polyphyllum* in Indian Western Himalayan region. *Reg Environ Chang* 21(2):1–11. <https://doi.org/10.1007/s10113-021-01763-5>
- Di Pasquale G, Saracino A, Bosso L, Russo D, Moroni A, Bonanomi G, Allevato E (2020) Coastal pine-oak glacial refugia in the Mediterranean basin: a biogeographic approach based on charcoal analysis and spatial modelling. *Forests* 11(6):673. <https://doi.org/10.3390/f11060673>
- Diaz HF, Grosjean M, Graumlich L (2003) Climate variability and change in high elevation regions: past, present and future. *Clim Chang* 59(1):1–4. <https://doi.org/10.1023/A:1024416227887>
- Elith J, Franklin J (2013) Species distribution modeling. In: *Encyclopedia of biodiversity*, 2nd edn. Elsevier, pp 692–705
- Fajardo J, Lessmann J, Bonaccorso E, Devenish C, Muñoz J (2014) Combined use of systematic conservation planning, species distribution modelling, and connectivity analysis reveals severe conservation gaps in a megadiverse country (Peru). *PLoS One* 9(12):e114367. <https://doi.org/10.1371/journal.pone.0122159>
- FAO, ITPS (2018) Global soil organic carbon map (GSOCmap) Technical Report, Rome, p 162
- Fick SE, Hijmans RJ (2017) WorldClim 2: new 1km spatial resolution climate surfaces for global land areas. *Int J Climatol* 37(12):4302–4315. <https://doi.org/10.1002/joc.5086>
- Fielding AH, Bell JF (1997) A review of methods for the assessment of prediction errors in conservation presence/absence models. *Environ Conserv* 24(1):38–49. <https://doi.org/10.1017/S0376892997000088>
- FSI (2019) India State of Forest Report 2019. Forest Survey of India, Ministry of Environment Forest and Climate Change, Government of India. Dehradun, India
- Gaur RD (1999) Flora of the District Garhwal. North West Himalaya. Transmedia, Srinagar
- GBIF (2022) GBIF occurrence download. <https://doi.org/10.15468/dl.rfwpc8>. Accessed 16 Apr 2022
- Grabherr G, Messerli B (2011) An overview of the world mountain environments. In: *Austrian MAB committee*, pp 8–14
- Hamid M, Khuroo AA, Charles B, Ahmad R, Singh CP, Araving NA (2019) Impact of climate change on the distribution range and niche dynamics of Himalayan birch, a typical treeline species in Himalayas. *Biodivers Conserv* 28:2345–2370. <https://doi.org/10.1007/s10531-018-1641-8>
- Hernandez PA, Graham CH, Master LL, Albert DL (2006) The effect of sample size and species characteristics on performance of different species distribution modeling methods. *Ecography* 29:773–785. <https://doi.org/10.1111/j.0906-7590.2006.04700.x>
- IPCC (2019) Summary for policymakers. In: Shukla PR, Skea J, Buendia EC, Masson-Delmotte V, Pörtner H-O, Roberts DC, Zhai P, Slade R, Connors S, van Diemen R, Ferrat M, Haughey E, Luz S, Neogi S, Pathak M, Petzold J, Pereira JP, Vyas P, Huntley E, Kissick K, Belkacemi M, Malley J (eds) *Climate change and land: an IPCC special report on climate change, desertification, land degradation, sustainable land management, food security, and greenhouse gas fluxes in terrestrial ecosystems*. In press
- Kaky E, Nolan V, Alatawi A, Gilbert F (2020) A comparison between Ensemble and MaxEnt species distribution modelling approaches for conservation: a case study with Egyptian medicinal plants. *Eco Inform* 60:101150. <https://doi.org/10.1016/j.ecoinf.2020.101150>

- Karger D, Conrad O, Böhner J, Kawohl T, Kreft H, Soria-Auza RW, Zimmermann NE, Linder HP, Kessler M (2017) Climatologies at high resolution for the earth's land surface areas. *Sci Data* 4: 170122. <https://doi.org/10.1038/sdata.2017.122>
- Kaushal S, Siwach A, Baishya R (2021) Diversity, regeneration, and anthropogenic disturbance in major Indian Central Himalayan forest types: implications for conservation. *Biodivers Conserv* 30(8):2451–2480. <https://doi.org/10.1007/s10531-021-02203-w>
- Kumar P (2012) Assessment of impact of climate change on Rhododendrons in Sikkim Himalayas using Maxent modelling: limitations and challenges. *Biodivers Conserv* 21(5):1251–1266. <https://doi.org/10.1007/s10531-012-0279-1>
- Kumar S, Stohlgren TJ (2009) Maxent modeling for predicting suitable habitat for threatened and endangered tree *Canacomyrica monticola* in New Caledonia. *Journal of Ecology and the Natural Environment* 1(4):094–098
- Malanson GP, Resler LM, Butler DR, Fagre DB (2019) Mountain plant communities: uncertain sentinels? *Prog Phys Geograp Earth Environ* 43(4):521–543. <https://doi.org/10.1177/0309133319843873>
- Manish K, Pandit MK (2019) Identifying conservation priorities for plant species in the Himalaya in current and future climates: a case study from Sikkim Himalaya, India. *Biol Conserv* 233:176–184. <https://doi.org/10.1016/j.biocon.2019.02.036>
- Manish K, Telwala Y, Nautiyal DC, Pandit MK (2016) Modelling the impacts of future climate change on plant communities in the Himalaya: a case study from Eastern Himalaya, India. *Model Earth Syst Environ* 2(92). <https://doi.org/10.1007/s40808-016-0163-1>
- McShea WJ (2014) What are the roles of species distribution models in conservation planning? *Environ Conserv* 41(2):93–96
- Morales-Barbero J, Vega-Álvarez J (2019) Input matters matter: bioclimatic consistency to map more reliable species distribution models. *Methods Ecol Evol* 10(2):212–224. <https://doi.org/10.1111/2041-210X.13124>
- Nakao K, Higa M, Tsuyama I, Matsui T, Horikawa M, Tanaka N (2013) Spatial conservation planning under climate change: using species distribution modeling to assess priority for adaptive management of *Fagus crenata* in Japan. *J Nat Conserv* 21(6):406–413. <https://doi.org/10.1016/j.jnc.2013.06.003>
- Nandy SN, Dhyani PP, Samal PK (2009) Resource information database of the Indian Himalaya. ENVIS Monograph 3:108
- Negi GCS (2022) Trees, forests and people: the Central Himalayan case of forest ecosystem services. *Trees For People* 8:100222. <https://doi.org/10.1016/j.tfp.2022.100222>
- Negi VS, Giri L, Sekar KC (2018) Floristic diversity, community composition and structure in Nanda Devi National Park after prohibition of human activities, Western Himalaya, India. *Curr Sci* 115(6):1056–1064
- Noce S, Caporaso L, Santini M (2020) A new global dataset of bioclimatic indicators. *Sci Data* 7(1): 1–12. <https://doi.org/10.1038/s41597-020-00726-5>
- Osorio-Olvera L, Lira-Noriega A, Soberón J, Townsend Peterson A, Falconi M, Contreras-Díaz RG, Martínez-Meyer E, Barve V, Barve N (2020) ntbox: an R package with graphical user interface for modeling and evaluating multidimensional ecological niches. *Methods Ecol Evol* 11:1199–1206. <https://doi.org/10.1111/2041-210X.13452>
- Pandit MK (2013) The Himalayas must be protected. *Nature* 501(7467):283–283. <https://doi.org/10.1038/501283a>
- Peterson AT, Papeş M, Soberón J (2008) Rethinking receiver operating characteristic analysis applications in ecological niche modeling. *Ecol Model* 213(1):63–72. <https://doi.org/10.1016/j.ecolmodel.2007.11.008>
- Peterson AT, Soberón J, Pearson RG, Anderson RP, Martínez-Meyer E, Nakamura M, Araújo MB (2011) Ecological niches and geographic distributions (MPB-49). Princeton University Press
- Phillips SJ (2017) A brief tutorial on maxent. Available from url: http://biodiversityinformatics.amnh.org/open_source/maxent/. Accessed 16 Apr 2022

- Phillips SJ, Duduk M, Schapire RE (2004) A maximum entropy approach to species distribution modeling. In: Proceedings of the twenty-first international conference on machine learning. ACM Press, pp 472–486. <https://doi.org/10.1145/1015330.1015412>
- Phillips SJ, Anderson RP, Schapire RE (2006) Maximum entropy modeling of species geographic distributions. *Ecol Model* 190(3–4):231–259. <https://doi.org/10.1016/j.ecolmodel.2005.03.026>
- Phillips SJ, Anderson RP, Dudík M, Schapire RE, Blair ME (2017) Opening the black box: an open-source release of Maxent. *Ecography* 40(7):887–893. <https://doi.org/10.1111/ecog.03049>
- Rai ID, Adhikari BS, Rawat GS, Bargali K (2012a) Community structure along timberline ecotone in relation to micro-topography and disturbances in Western Himalaya. *Not Sci Biol* 4(2):41–52
- Rai ID, Adhikari BS, Rawat GS (2012b) Floral diversity along sub-alpine and alpine ecosystems in Tungnath area of Kedarnath wildlife sanctuary, Uttarakhand. *Indian Forester* 138(10):927–940
- Rawal RS, Rawal R, Rawat B, Negi VS, Pathak R (2018) Plant species diversity and rarity patterns along altitude range covering treeline ecotone in Uttarakhand: conservation implications. *Trop Ecol* 59(2):225–239
- Rawat N, Purohit S, Painuly V, Negi GS, Bisht MPS (2022) Habitat distribution modeling of endangered medicinal plant *Picrorhiza kurroa* (Royle ex Benth) under climate change scenarios in Uttarakhand Himalaya, India. *Ecol Inform* 68:101550. <https://doi.org/10.1016/j.ecoinf.2021.101550>
- Rodríguez-Rodríguez D, Bomhard B (2011) Towards effective conservation in mountains: protected areas and biosphere reserves. In: Austrian MAB Committee (ed) Biosphere reserves in the mountains of the world excellence in the clouds? Austrian Sciences Academy
- Sanderson EW, Jaiteh M, Levy MA, Redford KH, Wannebo AV, Woolmer G (2002) The human footprint and the last of the wild: the human footprint is a global map of human influence on the land surface, which suggests that human beings are stewards of nature, whether we like it or not. *Bioscience* 52(10):891–904. [https://doi.org/10.1641/0006-3568\(2002\)052\[0891:THFATL\]2.0.CO;2](https://doi.org/10.1641/0006-3568(2002)052[0891:THFATL]2.0.CO;2)
- Schickhoff U, Bobrowski M, Böhner J, Bürzle B, Chaudhary RP, Gerlitz L, Heyken JL, Muller M, Scholten T, Schwab N, Wedegärtner R (2015) Do Himalayan treelines respond to recent climate change? An evaluation of sensitivity indicators. *Earth Syst Dynam* 6(1):245–265. <https://doi.org/10.5194/esd-6-245-2015>
- Schickhoff U, Singh RB, Mal S (2016) Climate change and dynamics of glaciers and vegetation in the Himalaya: an overview. In: Singh R, Schickhoff U, Mal S (eds) Climate change, glacier response, and vegetation dynamics in the Himalaya. Springer, Cham. https://doi.org/10.1007/978-3-319-28977-9_1
- Sharma CM, Tiwari OP, Rana YS, Krishan R, Mishra AK (2018) Elevational behaviour on dominance–diversity, regeneration, biomass and carbon storage in ridge forests of Garhwal Himalaya, India. *For Ecol Manag* 424:105–120. <https://doi.org/10.1016/j.foreco.2018.04.038>
- Singh P, Negi GCS (2018) Treeline species phenology: shoot growth, leaf characteristics and nutrient dynamics. *Trop Ecol* 59(2):297–311
- Singh JS, Singh SP (1987) Forest vegetation of the Himalaya. *Bot Rev* 53(1):80–192. <https://doi.org/10.1007/BF02858183>
- Singh CP, Panigrahy S, Thapliyal A, Kimothi MM, Soni P, Parihar JS (2012) Monitoring the alpine treeline shift in parts of the Indian Himalayas using remote sensing. *Curr Sci* 102(4):559–562
- Singh CP, Panigrahy S, Parihar JS, Dharaia N (2013) Modeling environmental niche of Himalayan birch and remote sensing based vicarious validation. *Trop Ecol* 54(3):319–327
- Singh U, Phulara M, David B, Ranhotra PS, Shekhar M, Bhattacharyya A, Dhyani R, Joshi R, Pal AK (2018) Static tree line of Himalayan silver fir since last several decades at Tungnath, western Himalaya. *Trop Ecol* 59:351–363
- Singh N, Tewari A, Shah S (2019) Tree regeneration pattern and size class distribution in anthropogenically disturbed sub-alpine treeline areas of Indian Western Himalaya. *Int J Sci Technol Res* 8(08):537–546

- Singh SP, Gumber S, Singh RD, Singh G (2020) How many tree species are in the Himalayan treelines and how are they distributed? *Trop Ecol* 61:317–327. <https://doi.org/10.1007/s42965-020-00093-7>
- Singh CP, Mohapatra J, Mathew JR, Khuroo AA, Hamid M, Malik AH (2021a) Long-term observation and modelling on the distribution and patterns of alpine treeline ecotone in Indian Himalaya. *J Geom* 15(1)
- Singh A, Samant SS, Naithani S (2021b) Population ecology and habitat suitability modelling of *Betula utilis* D. Don in the sub-alpine ecosystem of Great Himalayan National Park, North-Western Indian Himalaya: a UNESCO World Heritage site. *Proc Indian Natl Sci Acad* 87:640–656. <https://doi.org/10.1007/s43538-021-00055-0>
- Singh A, Samant SS, Naithani S (2021c) Population ecology and habitat suitability modelling of *Quercus semecarpifolia* Sm. in the sub-alpine ecosystem of Great Himalayan National Park, northwestern Himalaya, India. *S Afr J Bot* 141:158–170
- Siwach A, Kaushal S, Baishya R (2021) Terricolous mosses impact soil microbial biomass carbon and enzymatic activity under temperate forest types of the Garhwal Himalayas. *Environ Monit Assess* 193(8):1–14. <https://doi.org/10.1007/s10661-021-09295-5>
- Spiers JA, Oatham MP, Rostant LV, Farrell AD (2018) Applying species distribution modelling to improving conservation based decisions: a gap analysis of Trinidad and Tobago's endemic vascular plants. *Biodivers Conserv* 27(11):2931–2949. <https://doi.org/10.1007/s10531-018-1578-y>
- Srivastava V, Griess VC, Padalia H (2018) Mapping invasion potential using ensemble modelling. A case study on *Yushania maling* in the Darjeeling Himalayas. *Ecol Model* 385:35–44. <https://doi.org/10.1016/j.ecolmodel.2018.07.001>
- Swets JA (1988) Measuring the accuracy of diagnostic systems. *Science* 240(4857):1285–1293. <https://doi.org/10.1126/science.3287615>
- Tariq M, Nandi SK, Bhatt ID, Bhavsar D, Roy A, Pande V (2021) Phytosociological and niche distribution study of *Paris polyphylla* smith, an important medicinal herb of Indian Himalayan region. *Trop Ecol* 62(2):163–173. <https://doi.org/10.1007/s42965-020-00125-2>
- Tiwari OP, Rana YS, Krishan R, Sharma CM, Bhandari BS (2018) Regeneration dynamics, population structure, and forest composition in some ridge forests of the Western Himalaya, India. *For Sci Technol* 14(2):66–75. <https://doi.org/10.1080/21580103.2018.1447517>
- Ugupta S, Sharma J, Jayaraman M, Kumar V, Ravindranath NH (2015) Climate change impact and vulnerability assessment of forests in the Indian Western Himalayan region: a case study of Himachal Pradesh, India. *Clim Risk Manag* 10:63–76. <https://doi.org/10.1016/j.crm.2015.08.002>
- Uttarakhand at a Glance (2020) Uttarakhand at a Glance 2018-19. Directorate of Economics and Statistics, Department of Planning, Government of Uttarakhand, Dehradun
- Veloz SD (2009) Spatially autocorrelated sampling falsely inflates measures of accuracy for presence-only niche models. *J Biogeogr* 36(12):2290–2299. <https://doi.org/10.1111/j.1365-2699.2009.02174.x>
- Wani IA, Verma S, Kumari P, Charles B, Hashim MJ, El-Serehy HA (2021) Ecological assessment and environmental niche modelling of Himalayan rhubarb (*Rheum webbianum* Royle) in northwest Himalaya. *PLoS One* 16(11):e0259345. <https://doi.org/10.1371/journal.pone.0259345>
- WCS—Wildlife Conservation Society, and Center for International Earth Science Information Network—CIESIN—Columbia University (2005) Last of the wild project, version 2, 2005 (LWP-2): Global Human Influence Index (HII) Dataset (Geographic). NASA Socioeconomic Data and Applications Center (SEDAC), Palisades, New York. <https://doi.org/10.7927/H4BP00QC>. Accessed 16 Apr 2022
- Yadava AK, Sharma YK, Dubey B, Singh J, Singh V, Bhutiyani MR, Yadav RR, Misra KG (2017) Altitudinal treeline dynamics of Himalayan pine in western Himalaya, India. *Quat Int* 444:44–52. <https://doi.org/10.1016/j.quaint.2016.07.032>

- Yang XQ, Kushwaha SPS, Saran S, Xu J, Roy PS (2013) Maxent modeling for predicting the potential distribution of medicinal plant, *Justicia adhatoda* L. in Lesser Himalayan foothills. *Ecol Eng* 51:83–87
- Yoon S, Lee WH (2021) Methodological analysis of bioclimatic variable selection in species distribution modeling with application to agricultural pests (*Metcalfa pruinosa* and *Spodoptera litura*). *Comput Electron Agric* 190:106430. <https://doi.org/10.1016/j.compag.2021.106430>
- Zhang D, Rushforth K, Katsuki T (2011) *Abies spectabilis*. The IUCN red list of threatened species 2011: e.T42300A10686224. <https://doi.org/10.2305/IUCN.UK.2011-2.RLTS.T42300A10686224.en>
- Zhang MG, Zhou ZK, Chen WY, Slik JF, Cannon CH, Raes N (2012) Using species distribution modeling to improve conservation and land use planning of Yunnan, China. *Biol Conserv* 153: 257–264. <https://doi.org/10.1016/j.biocon.2012.04.023>
- Zisenis M, Price MF (2011) Europe's mountain biodiversity: status and threats. In: Austrian MAB Committee (ed) Biosphere reserves in the mountains of the world excellence in the clouds? Austrian Sciences Academy